

# Ultra stable oscillators dedicated for space applications: oscillator and quartz material behaviors vs radiation

Gilles CIBIEL

Microwave and Time-Frequency Dept.  
Centre National d'Etudes Spatiales (CNES)  
Toulouse - France  
[gilles.cibiel@cnes.fr](mailto:gilles.cibiel@cnes.fr)

Bruno BOIZOT

Laboratoire des solides irradiés (LSI)  
Ecole Polytechnique/CEA/CNRS (UMR7642)  
Palaiseau - France

Jean-Jacques BOY, Jean-François CARLOTTI  
ENSMM, LCEP Dept.  
FEMTO-ST institute  
Besançon - France

Olivier CAMBON, Sabine DEVAUTOUR-VINOT  
LPMC Dept.  
Université de Montpellier II  
Montpellier - France

Vincent CANDELIER, Jacques LAMBOLEY  
R&D Dept.  
C-MAC Frequency Product  
Argenteuil - France

Pierre GUIBERT, Alain LARGETEAU  
CRP2A / ICMCB Dept.  
Université de Bordeaux  
Bordeaux - France

Christophe INGUIMBERT  
DESP Dept.  
ONERA-CERT  
Toulouse - France

Delphine PICCHEDA  
Quartz Dept.  
GEMMA - SOROME  
Annecy - France

**Abstract**—This paper presents the first results obtained in the R&D study initiated by the CNES at the end of 2004. Numerous French experts have been gathered to determine and to tentatively understand the mechanisms responsible for the radiation sensitivity of quartz resonators and to correlate the results of various analyses in order to reduce or to anneal their susceptibilities.

## I. INTRODUCTION

Ultra stable oscillators (USO) are widely used in space systems (telecommunication, navigation, precise positioning). And for all space programs need to verify the end-of-life (EOL) frequency stability over the lifetime (from few years up to 20 years), as well as the mid and short-term stabilities and the phase noise. These specifications should be compliant with all on-board environmental conditions, mainly temperature, magnetic fields from earth or spacecraft, and radiations. The present paper is focused on this last issue.

Previous works have showed that radiation sensitivity of USO is due to the quartz resonator. The frequency fluctuations depend on resonator technology, quartz crystal quality (impurities, dislocations...) and radiation characteristics. Up to now, some works concerned only quartz-material radiation sensitivity and other ones discussed just on resonator/oscillator radiation sensitivity. Nevertheless, few published works have investigated the

correlation between both aspects: quartz material and quartz resonator/oscillator radiation-sensitivity. Reference [WEA04] of Applied Physics Laboratory from John Hopkins University summarizes prior works and presents some interesting results (not discussed here).

CNES (French space agency) started at the end of 2004 a R&D study taking into account quartz material and oscillator. French experts in quartz material (GEMMA, ICMCB-CRPAA, LCEP, LPMO) in quartz resonator (C-MAC, LCEP), in quartz oscillator (C-MAC, LCEP, LPMO) and in radiation (CPO, LSI, ONERA) have been gathered to determine and understand the mechanisms responsible for the radiation sensitivity of material, resonator and oscillator, and to correlate them in order to reduce their susceptibilities.

First part of this paper highlights experience-returns of on-board USO and proposes short-term solutions to reduce radiation sensitivity. The second part is a summary of the preliminary R&D results.

## II. OSCILLATOR BEHAVIOR VS RADIATION

### A. DORIS Program

One of major programs concerned by the radiations problem is DORIS (Doppler Orbitography and Radiopositioning Integrated in Space). It is Doppler satellite tracking system developed for precise determination and

precise ground location. Its ultimate aim is to achieve an accuracy of one centimetre. The DORIS system was designed by CNES, the French space agency, in partnership with French mapping and survey agency IGN and space geodesic research institute GRGS, to answer to the one centimetre challenge. Since 1990, it is on-board of JASON1 and ENVISAT altimetric satellites and remote sensing satellites SPOT series: 2, 4 and 5. SPOT series and ENVISAT are at 830 km, and JASON1 at 1336 km. Altitudes correspond to low Earth orbit (LEO). It also flew with SPOT3 and TOPEX-POSEIDON. Future DORIS will be embarked on JASON2, PLEIADES, ALTIKA, HY2... Currently, seven DORIS instruments are in orbit, based on a one-way bi-frequency Doppler technique with on-board very accurate measurements from a network of 55 ground transmitters beacons.

### B. Radiation effects

Radiation effects responsible of a frequency shifts on space USO are caused by two main sources: space radiation due to cosmic rays, trapped protons, and electrons in the Van Allen belts or solar flare protons ejected from the sun during solar activity.

#### 1) Van Allen belts

The Van Allen belts are toroidal belts of charged particles surrounding the Earth near the equator. There are two belts: the inner belt, which extends to about 45° North and South geomagnetic latitude and from 800 to 8,000 km in altitude, and the outer belt, which fluctuates in size and intensity with solar activity, but is symmetrical about the equator and extends to about 70° geomagnetic latitude North and South and reaches altitudes up to 130,000 km. Results from previous investigations also showed that cosmic rays consist primarily in high energy protons with too small fluxes to produce radiation effects in quartz crystals [VIG94], [SUT88]. Stassinopoulos and Barth [STA84] showed also that trapped electrons in the Van Allen belts do not contribute significantly to the total radiation dose accumulated by spacecrafsts in LEO. Therefore, studies on the susceptibility of quartz crystal resonators to LEO radiation environment focus on proton radiation induced effects.

Van Allen belts effects on on-board USO are determined by several parameters: duration of the mission, orbit parameters... and, finally, a 3-D Monte-Carlo analysis of the geometrical and physical description of the satellite taking into account the equipment and the USO itself [BRU05] is necessary to calculate the radiation sensitivity of the USO.

The protons able to go into the quartz crystal are those whose energy is greater than 60 MeV. Figure 1 gives the spatial distribution of such protons in the belt at the JASON1 orbit altitude where the usual SAA (South Atlantic Anomaly) region is visible. Nevertheless, we observed the presence of significant flux in wide intervals of longitudes and latitudes after the East and West sides of SAA. The

resulting radiation orbital cycle is about 1 rad/h<sup>1</sup> during 10 min to 40 min on a 120 min cycle.

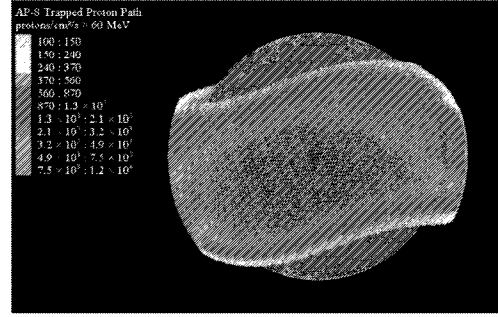


Figure 1. Figures (proton) : Integral protons belt flux for energies greater than 60 MeV in the usual SAA region at the East and the West.

All the DORIS USO are in the inner belt. In fact, they are affected by three main effects: the total ionizing dose (TID), the low dose rate (LDR) and the single event (SE).

#### 2) Total ionizing dose

The TID is the main parameter affecting the EOL frequency stability. For example, USO for applications such as telecommunication or precise positioning need respectively an EOL frequency stability of 0.2 to 1 ppm over 20 years and 0.2 ppm over 5 to 10 years.

Using some ground beacons synchronized by an atomic frequency standard, it is possible to determine the on-board USO frequency over one pass with an uncertainty of a few 10<sup>-12</sup>. The DORIS EOL and mid-term (MT) required performances in orbit are compliant for each USO, except for JASON1, where large frequency variations are observed (Figure 1).

In fact, the TID effect is mainly due to the accumulation of LDR of ionizing radiations and single events.

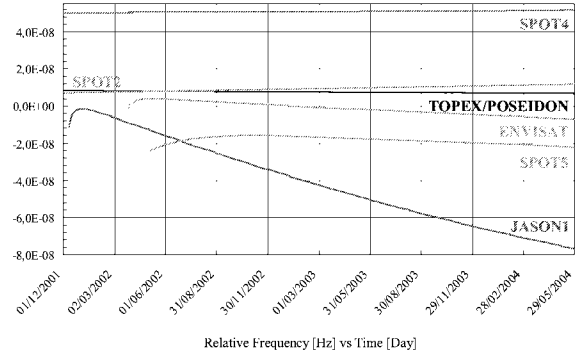


Figure 2. Long-term (LT) frequency instability (aging) of 10 MHz DORIS in-flight USO in LEO: SPOT series (2,4,5) ENVISAT at 830 km orbit altitude, TOPEX-POSEIDON and JASON1 at 1336 km altitude.

#### 3) Low dose rate ionizing radiation

Figure 3 presents the frequency variations of the DORIS USO observed in July 2002 and April 2003 on-board

<sup>1</sup> 1 Gy = 100 rad

JASON1 satellite over a period of 4 days. The observed discontinuous frequency variations ( $1$  to  $6.10^{-11}$  peak-to-peak) are strongly correlated to the run of the satellite through the SAA. The radiation environment of LEO corresponds to radiation exposures with relaxation periods. The flux of protons during orbit is not continuous. Cycles coincide with transits through the SAA proton belt.

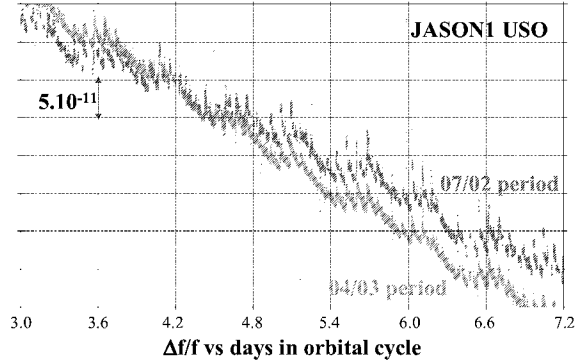


Figure 3. Frequency variations of the DORIS USO observed in July 2002 and April 2003 on-board JASON1 satellite over a period of 4 days.

#### 4) Single events : Solar flares

Solar flare protons ejected from the sun during solar activity induce also frequency variations. Figure 4 illustrates the frequency drift of on-board DORIS USO caused by the solar flare observed the 20<sup>th</sup> of January 2005.

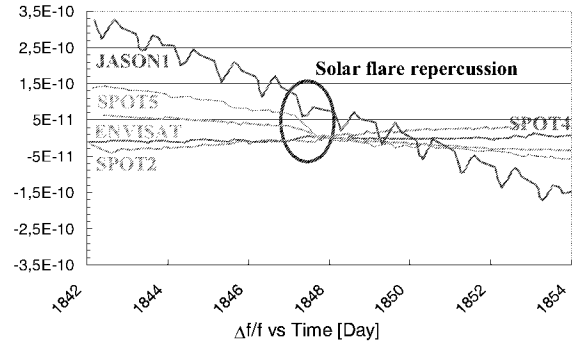


Figure 4. Solar flare on frequency variations of DORIS on-board USO.

The high particles rates from solar flare are transitory with intensity peaking of  $100$  to  $10,000$  particles  $\text{cm}^{-2}\text{s}^{-1}$ .

### C. Solutions

#### 1) Radiation shielding

The quartz crystal resonators can be shielded from some radiation characteristics by metals such as aluminium or copper or by composite materials lead but weight considerations in spacecraft often make the addition of shields prohibitive. Furthermore, high energy protons cannot be effectively shielded.

#### 2) Specific quartz materials

Most of works have demonstrated that quartz impurities quantities have a important role in radiation susceptibility (for both low and high radiation levels). A few suppliers (GEMMA, SAWYER, VNIISIMS) and laboratory (HIRST-GEC ASTRUM) have dedicated quartz crystals to low radiation sensitivity applications. However, even if these materials present about the same trace elements, the frequency deviation signature and magnitude are not the same. Figure 5 presents the frequency behaviour of some USO manufactured with high quality quartz crystals on-board of TOPEX-POSEIDON, JASON1, and JASON2. A  $\gamma$ -ray beam of  $1$  rad/h flux was applied during 40mn every 120mn.

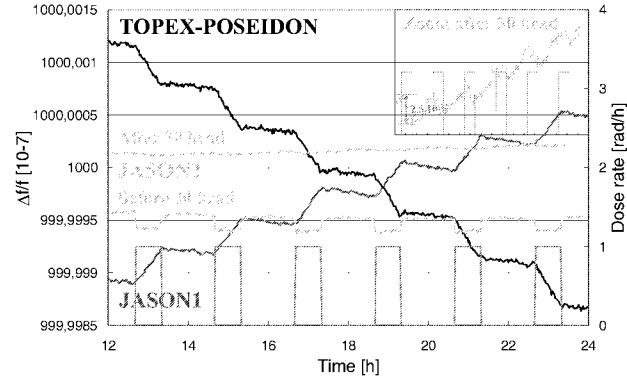


Figure 5. Frequency behaviour of some USO on-board of TOPEX-POSEIDON, JASON1, and JASON2 quartz-lots

The TOPEX-POSEIDON and JASON1 quartz materials have a similar behaviour. The main radiation mechanisms are due to cumulated dose. Their frequency changes are of  $5.10^{-11}$  and  $2.10^{-11}$  respectively for  $1$  rad cumulated dose. On the other hand, the quartz foreseen to be used in JASON2 is sensitive to the flux dose ( $2.5.10^{-11}$  at  $1$  rad/h). Contrary to the other batches, JASON2 quartz is unswept. The amount of protons or alkali ions is the same than as-received.

Frequency deviation-signature and magnitude of each quartz lots are almost different. Moreover in the same lot, a non-negligible scattering has been observed:

- TOPEX lot:  $-8.10^{-11}$  to  $-1.10^{-12}$
- JASON1 lot:  $2.10^{-10}$  to  $5.10^{-12}$
- JASON2 lot:  $5.10^{-11}$  to  $1.10^{-12}$

Such a scattering forces on-board USO manufacturer to evaluate LDR radiation performance of each quartz crystal of a production batch. Furthermore, this heavy operation does not guarantee the low LDR sensitivity.

#### 3) Pre-conditioning

Fortunately, it has been noted that a pre-irradiation of resonators can reduce radiation induced frequency shifts [NOR84]. Indeed, C-MAC Frequency Products has investigated some high quality quartz materials coming from VNIISIMS, SAWYER, and GEMMA [CAN01]. The

authors said that only one type of material seems to be saturated after 150 krad (which has been also swept) whereas the others are saturated after only 5 to 20 krad.

According to these results, the authors decide to apply a 30 krad pre-conditioning on the quartz crystal material (GEMMA) for the next JASON on-board USO generation (JASON2).

The result is translated by an impressive improvement of magnitude of more than one decade. Moreover, the resonators pre-conditioning of quartz crystal lot modify the LDR sensitivity. After this pre-irradiation, the cumulated dose becomes the main cause of frequency drift.

Furthermore, it has been observed that the LDR susceptibility of quartz crystal resonators submitted to 30 and 60 (30+30) krad is greatly reduced up to a ratio of 20. But, unfortunately, the first 30 krad irradiation degrades the Short Term stabilities of all oscillators (except one) (Figures 6 and 7). Up to now, this degradation has not been explained. The second 30 krad conditioning dose consists in an EOL qualification of the first dose. It corresponds to about twice the total life ionizing dose in orbit (15 krad) and does not decrease the performances of the USO.

Even if the pre-conditioning allowed to improve the LDR sensitivity up to one decade and more, this step of the USO development is very heavy : one pre-conditioning (30 krad), one EOL radiation qualification and three LDR radiation campaigns (before and after 30 krad pre-conditioning).

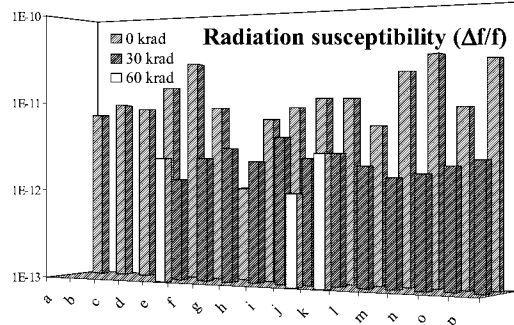


Figure 6. LDR susceptibility of quartz crystal resonators lot dedicated for JASON2 USO before and after 30 and 60 krad irradiation

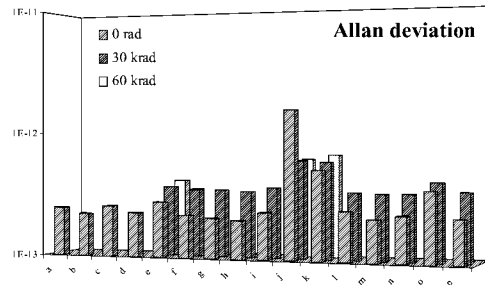


Figure 7. Short term (ST) frequency instability of quartz crystal resonators lot dedicated for JASON2 USO before and after 30 krad.

The next step consists now in understanding the main quartz mechanisms inducing frequency shifts and the second part summarizes our first investigations to reach these goals.

### III. MATERIALS BEHAVIOUR VS RADIATION

To understand the interactions between quartz crystal and resonant frequency shift due to irradiations, it is necessary first to know in-depth the quartz crystal itself. For that, we have to qualify and, if possible, to quantify the defects present in the lattice of the crystal. They can be microscopic point or line defects if the macroscopic defects as inclusions, veils or twins do not be taken into account. We have numerous tools to measure first the amount of imperfections in the crystal but also their displacements or recombinations under irradiations.

So, we present here the results obtained by a variety of analytical techniques such as chemical analysis (ICP-AES) for metallic impurities, low temperature FTIR, X-ray topography for dislocations, dielectric relaxation spectroscopy for charges dynamics, EPR measurements for paramagnetic defects, micro Raman spectroscopy, and, last, thermoluminescence. A brief description of each kind of measurements is also included.

#### A. Investigated quartz materials

##### 1) Manufactured data:

First of all, we had to choose different kinds of quartz materials to try to obtain a large spectrum of defects with their own environment. So, we introduce in our batch some samples of Natural quartz (noted "N") and synthetic quartz coming from 4 different suppliers: GEMMA (from France), SAWYER (from USA), VNISSIMS (from Russia) and HIRST-ASTRIUM (kindly offered by Angus Haston and grown in UK). These samples are called S1, S2, S3 and S4 (no correlation with previous order). In each quartz block, we have prepared, whenever, samples with the same orientations and the same dimensions except for those used in measurements is possible normalized (Y-cut samples for IR spectrometry and X-ray topography).

##### 2) Low temperature FTIR:

All crystalline quartz blocks contain impurities randomly incorporated during the growth. The dominant impurity in natural and in hydrothermally grown quartz crystal is aluminium as  $Al^{3+}$  cation substituting for  $Si^{4+}$ . An aluminium ion requires additional positive charge compensator, such as  $Li^+$ ,  $Na^+$ ,  $K^+$  or proton ( $H^+$ ) to maintain charge neutrality. The impurities and its compensators give rise to aluminium-hydroxyl ( $Al-OH^-$ ) or aluminium-alkali ( $Al-M^+$ ) or aluminium-hole (hole trapped at an adjacent oxygen site named  $Al-h^+$ ) defect centers. In addition to the  $Al$ -related centers, there are other types of point defects also present in quartz: oxygen vacancies, numerous  $OH^-$  molecules formed by protons trapped on oxygen atoms near unidentified point defects in the lattice (Fe, Ti, Ge, Ca...). The main effect produced by irradiation of unswept quartz

at room temperature or above is the conversion of Al alkali centers into a mixture of Al-hole and Al-OH. Electrodiffusion under high temperature and high voltage (called “sweeping”) realized to ionize and to extract monovalent impurities can be performed under vacuum or in air. In the last case, all Al-alkali are dissociated to form Al-OH<sup>−</sup>. Under vacuum, Al-hole can be created (BAH99) [MAR96].

One of the first techniques used to characterize these point defects is the infra-red spectrometry. Indeed, the lattice defects and impurities cause infra-red absorption bands around 3400 cm<sup>−1</sup>. Most of them are due to hydrogen vibrations. Figures 8 and 9 illustrate this purpose by the presentation of 3 IR spectra made on Y-cut samples, with 2 polished faces and a thickness of about 5 mm. The first one (Figure 8), which concerns Natural quartz, exhibits some sharp bands revealing the strong presence of OH ions, particularly by a deep absorption at 3378 cm<sup>−1</sup>. Furthermore, the peak existing at 3480 cm<sup>−1</sup> has been attributed by Dodds and Fraser to a high level of Lithium. This absorption continues to appear even if the quartz undergoes a high level of radiation.

On the 2 other spectra (Figure 9), the presence of the 4 sharp absorption bands, called s<sub>1</sub> to s<sub>4</sub>, indicates a synthetic origin for the samples which are, as previously, 5 mm thick Y-cut plates. These bands are attributed to the hydroxyl ions trapped during the growth and called GD-OH (OH-related growth defect bands). For high quality quartz (as S1 and S2), only the s<sub>4</sub> band is well resolved at room temperature [MAR02].

We show below how the height of the “s” bands is modified by the ionizing radiation and how new absorption bands appear. These e<sub>1</sub> and e<sub>2</sub> absorptions, located at 3306 and 3366 cm<sup>−1</sup>, correspond to vibrations of the OH link in the Al-OH groups. The radiations are  $\gamma$  rays coming from <sup>60</sup>Co source.

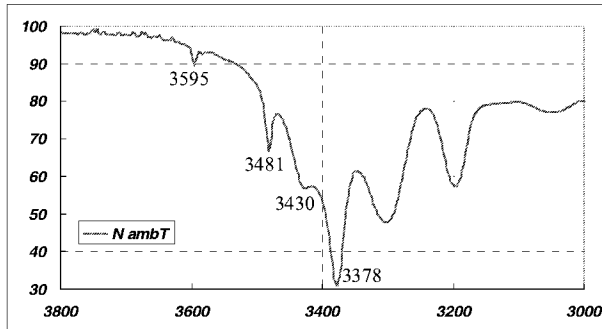


Figure 8. transmission level (in arbitrary units) vs wave length in natural quartz at ambient temperature.

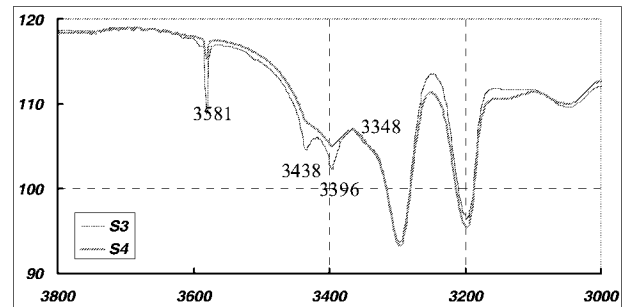


Figure 9. transmission level (in arbitrary units) vs wave length in S3 and S4 synthetic quartz at nitrogen liquid temperature (before radiation).

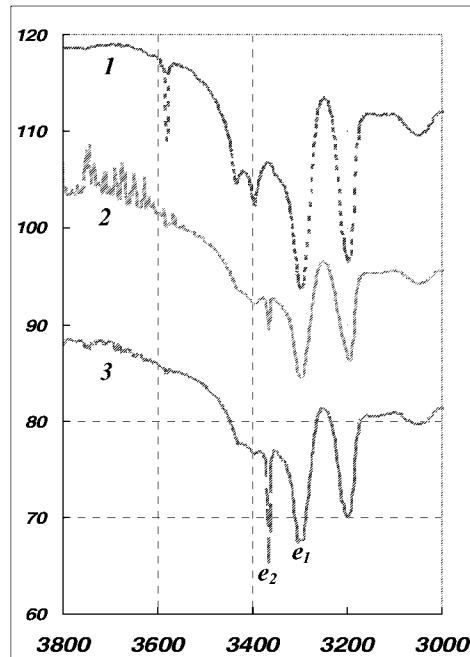


Figure 10. IR transmission for S3 sample before irradiation (1), after 100 krad (2) and 1 Mrad (3).

### 3) Chemical analysis:

Up to now, to quantify the content of foreign atoms in the quartz crystal lattice, we use ICP-AES (Inductively Coupled Plasma - Atomic Emission Spectrometry) technique. It is a photometric method using plasma at temperatures in the range 6,000-10,000 K. At these temperatures, each element is excited and emits characteristic photons. ICP is a discharge without electrodes in a gas at atmospheric pressure, maintained by the energy provided from a high frequencies generator. The limits of detection are very low (but different for one element to another one) and to improve the reliability of the measurements, it is also possible to use several emission bands for each element.

Measurements are made on a sample which lattice ( $\text{SiO}_2$ ) is dissolved in hydrofluoric acid in order to keep only the foreign atoms. During this operation, the risks of pollution are very detrimental: Accidental pollution is not always detectable when it is weak. It can modify certain results. To minimize all these uncertainties, every solution (standard and blank) has to be prepared simultaneously with the sample. Under these conditions, pollution by the chemicals used for the preparation of the solutions will then be reduced to the minimum. But, because of the very low contents observed in certain crystals (less than a few tenth of ppm weight of aluminium and a few tens of ppb of Lithium), we are too close to the limits of detection and the blank and the solution can contain almost the same impurities levels.

The following table, presenting the results of  $2 \times 2$  samples of synthetic quartz and one natural, shows that S1 and S2 quartz crystal exhibit very low levels on Al and Li and differ from the 2 others named S3 and S4.

TABLE I. CHEMICAL ANALYSIS

ppm weight	Al	Fe	Ca	Li	Na	K
S1 / S2	1.2/2	2.2/1	8/7	0.2/0.1	4.5/1.3	4/4
S3 / S4	5/6	2/5	22/26	0.6	7/10	9/11
N	8	1.2	3.2	1.6	1.3	0.5

Regarding these results, we decide to use another technique avoiding the phase of dissolution. We are now evaluating the Glow Discharge Mass Spectrometry. Used as High Resolution method, the HR-GDMS is an extremely powerful technique for the analysis of all trace and ultra-trace elemental constituents of inorganic materials. Samples are analyzed in solid form and so do not require the laborious and complicated dissolution methods inherent with such techniques as ICP – AES or AAS. In addition, GDMS does not suffer from the extreme matrix dependence of most other elemental analysis techniques, minimizing the need for matrix matching standards. Its principle involves the atomization of a solid sample by sputtering in a low-pressure DC plasma. The sputtered atoms are then ionized in the plasma and extracted into the mass analyzer for separation and detection. In accordance of the first results, we hope to obtain very low levels of Al atoms, about a few hundredth of ppm weight.

#### 4) X-rays topography:

To illustrate this type of control, we present here below 3 topographies made on the [2-1.0] reticular plane of Y-cut samples from S1 and S2 for the first ones and N for the third. As usually, we do not observe any dislocation in the natural quartz, but a few of them are present in the synthetic slices.

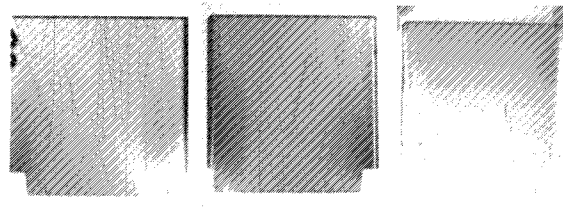


Figure 11. Topographies on quartz samples, respectively S1, S2 and N.

#### 5) Dielectric Relaxation Spectroscopy:

Dielectric Relaxation Spectroscopy is a powerful tool to study charges dynamics in solids. The dielectric response can be regarded as arising from the dipolar reorientation associated to electric charges hops within short distances. The dielectric relaxation phenomenon is then ascribed to charges hopping above the potential barriers that separate the different crystallographic positions. This approach has already been applied to study the different qualities of quartz [JEA92] and the radiation effects in quartz material [FOT73, SEM85]. This approach has been applied to different materials [DEV99].

The dynamics of ionic charges confined in quartz materials, using a Broadband Dielectric Spectrometer Novocontrol have been investigated. Ionic displacements are evaluated from the measurement of the imaginary part of the dielectric constant  $\epsilon''$ , under the application of an ac electric field at a constant frequency (0.02 Hz) and under variations of the temperature in the range [25, 250°C]. The pure dielectric response is recorded whereas PTFE blocking electrodes are inserted between the sample and the metallic electrodes of the impedance-meter. The samples are circular SC-cut plates with a thickness of 0.5 mm between polished faces. The evolution of  $\epsilon''$  as a function of the temperature is reported in Figure 12. It differs according to the quality of the studied quartz. In each case, the signal does not exhibit Debye behaviour, but is rather broad, revealing the existence of a distribution of the relaxation times, whatever the sample under investigation.  $\epsilon''$  peaks appear in temperature according to the following sequence: N < S1 < S3 ≈ S4 ≈ S2 (Table II). This trend is a signature of the quality of the quartz under investigation, implying that charge carriers in the natural quartz are more mobile than in the synthetic ones.

TABLE II. TEMPERATURE POSITION OF THE MAXIMUM OF THE RELAXATION PEAK IN FUNCTION OF THE NATURE OF THE QUARTZ.

Samples	Tmax of relaxation peak (°C)	
	before irradiation	after 100krad
N	80	47
S1	125	54
S2	161	91
S3	171	62
S4	169	75

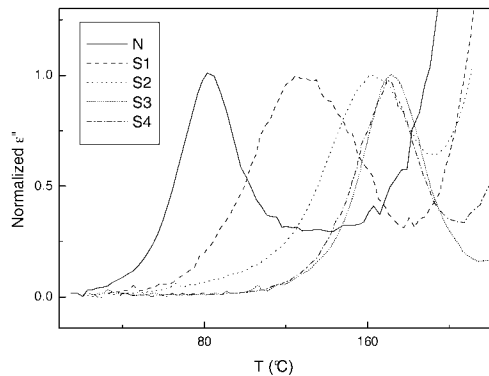


Figure 12.  $\epsilon''$  evolution of the different quartz before irradiation exposure

Further experiments have been undertaken in order to understand the effect of 100krad gamma irradiations on the different quartz materials (Figure 13).

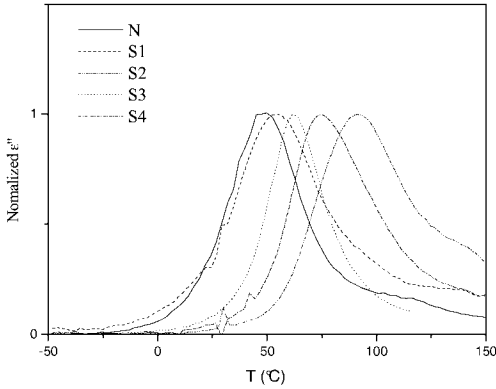


Figure 13. evolution of  $\epsilon''$  after 100krad irradiation exposure

For all samples, the dielectric peak shift to the lower temperatures is observed (Table II). This implies that the mobility of the charge carriers is increased by the radiations, which modifies the structure of the material. These modifications tend to decrease the potential barrier that the charge carriers have to reach. After irradiation, all the  $\epsilon''$  peaks appear in a temperature range smaller than before irradiation. The effect of the radiation is to modify the different initial structures to a similar structure that presents quite similar charge carriers mobility. However some discrepancies can be observed: the sequences of the  $\epsilon''$  peak position in temperature becomes  $N < S1 < S3 < S4 < S2$ . The sample N remains the one which contains the more mobile charge carriers. On the opposite, the quartz S2 contains the less mobile charge carriers after irradiation ( $T_{\max} = 91^\circ\text{C}$ ). In a near future, we aim to investigate the effect of the radiation dose and the temperature curing.

#### 6) *In situ* UV-visible absorption measurements:

We have first studied the transitory process of defects creation using *in situ* UV-visible absorption measurements during a  $\beta$ -irradiation. The effect of dose from  $10^8$  to  $10^{11}$  rad have been also studied by Electron Paramagnetic Resonance (which can give information on nature and content of defects) and micro Raman spectroscopy (which analyses the structural changes of the quartz at microscopic scale). The second important point of this work about irradiation effect is that trace elements should not be the only parameter guiding defect creation processes. Indeed, we have to consider also the homogeneity of material at the micrometric scale in terms of impurities speciation and structural fluctuations on Silicon tetrahedral environment for example. Spatial analysis of quartz samples by micro Raman spectroscopy have therefore been conducted first on as-grown quartz sample in order to characterize the structural homogeneity before irradiation and after irradiation in order to detect possible migration and segregation of impurities.

Raman spectra were recorded on a Renishaw microspectrometer using the 514.5 nm line of an  $\text{Ar}^+$  laser. Experiments were carried out through a  $\times 100$  Olympus objective with a laser power of 20 mW on the sample. Spatial resolution obtained with the confocal configuration is about  $10 \mu\text{m}^3$ .  $\beta$ -irradiation was performed by using a Van de Graff electron accelerator (2.5 MeV, 1  $\mu\text{A}$ ) on the different SC-cut samples shaped with squared surfaces of  $15 \times 15 \text{ mm}^2$  optically polished and a thickness of 0.5 mm. In-situ absorption measurements during the irradiation were done in the spectral range 1.5-6.0 eV by using two lamp sources, one halogen and one deuterium, and a prism-based detection system equipped with a CCD camera. The irradiation-detection system was arranged by a 45 degrees mounting of the samples larger surface with respect to the detection light direction and 90 degrees with respect to the irradiation direction.

#### 7) Synthesis of the results obtained by Micro Raman:

Before irradiation, the results obtained by micro Raman spectroscopy mapping of the different quartz samples show that this method is able to detect, on synthetic quartz, structural heterogeneities at a microscopic scale correlated with the presence of luminescence signal of impurities and modification in silicon tetrahedral environment. *In situ* UV-visible absorption measurements on the samples previously studied by micro Raman show first that, during irradiation, a transitory defect ( $\text{E}'$  center) is produced. The second important point of this *in situ* work is that the defects produced almost disappear once irradiation is stopped. Moreover the relaxation behaviour of defect content is long and therefore is controlled by the impurities diffusion in quartz samples. This result could therefore be correlated with the changes in oscillating properties of quartz samples in space environment. Finally, we suppose that the content of defects produced during the irradiation depends on the homogeneity at the microscopic scale observed on quartz

samples by Raman spectroscopy. Post mortem studies versus irradiation dose ( $10^8$  to  $4.10^{11}$  rad) and Raman confirm first by EPR measurements the strong reversible process of defect creation in quartz under irradiation. Raman study on irradiated quartz shows finally that the structure of quartz material is not changed at lower dose and that the structural changes occur at doses higher than  $10^{11}$  rad.

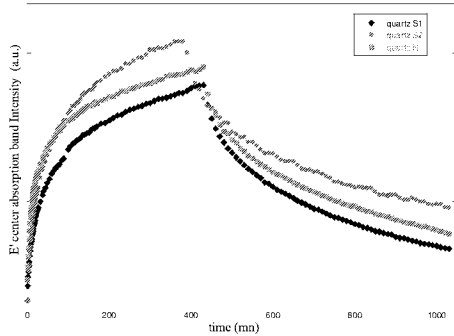


Figure 14. Evolution of the concentration of  $E'$  center versus time for S1, S2 and N

### 8) Thermoluminescence: Material and instruments

The analyses reported were carried out on SC-cut quartz discs (diameter 9mm, thickness 0.5 mm). For each type of material, 4 samples were studied, respectively not irradiated, and irradiated by 100 krad, 1 Mrad and 10 Mrad  $\gamma$  doses from  $^{60}\text{Co}$  source before the thermoluminescence (TL) study.

The TL device used (built at the IRAMAT-CRP2A laboratory) allows us to record the luminescence signals from approximately room temperature to 500°C in a nitrogen (gas) atmosphere and at a constant heating rate (about 2°C/s). The spectral window (350-450 nm) was selected by optical filters (2 Schott BG12) and the phototube type (EMI 9813 QKA). The following 4-step protocol has been applied to each disc:

1. first heating of as received material;
2. second heating (to determine the zero level of TL or the residual plus electronic background signal);
3. Irradiation by a 1 krad beta dose and third heating starting 2 minutes after the end of irradiation (with a  $^{90}\text{Sr}$ - $^{90}\text{Y}$  source delivering 7 rad/s);
4. fourth heating (same as step 2).

The TL experiments lead us to sort the high dosed (100 krad, 1 Mrad and 10 Mrad) quartz material into 3 types according to their behaviours: i) Natural, ii) S1 and S3, iii) S2 and S4. Figure 15 shows the TL curves obtained from the 100 krad samples. By comparison with synthetic quartz, the TL intensity of N is particularly high within the 150-500°C range: a shoulder due to a component situated at 180°C and maxima at 230, 315, 420°C are observed. The

TL of S1 and S3 presents some similarities with N, but with intensity 20 times lower (maxima at 230, 320-340°C). In the contrary, they exhibit a strong broad emission around 470°C. The TL of S2 and S4 is very low, with maxima of TL between 150 and 250°C.

At very high doses, the evolution of TL with dose is irregular. Considering the high temperature components of TL (higher than 300°C), the signal intensity evolves without any clear relationship with the dose applied: the TL of N and S2 grows, although that of S1 reaches a maximum at 1 Mrad. Inversely, low temperature TL emissions of all synthetic crystals tend to decrease with dose (dose-quenching effects, a propensity to induce non radiative charge recombinations). Moreover, a shift towards higher temperature of TL maxima is observed with S1 at 10 Mrad.

At low doses (1 krad), there is no similarity among the non-Previously irradiated quartz samples (Figure 15). We only note that N presents the highest intensity of the 110°C peak. All samples have low temperature components (below 250°C) with similar intensities. Above 300°C, N and S1 exhibit meaningful TL emissions.

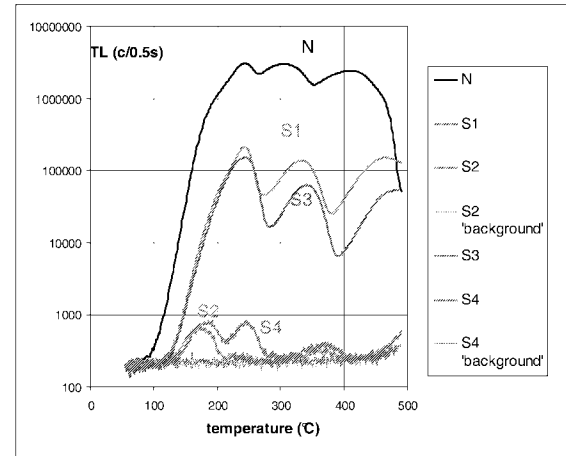


Figure 15. : TL response of natural (N) and synthetic quartz (S1 to S4) irradiated by 100 kard.

All materials exhibit a 110°C peak of which lifetime is around 1 hour at room temperature. According to the actual interpretations of luminescence, it would be an evidence for the radiative de-excitation of an Al center (in substitution for Si) charge-compensated by an alcali ion (Al-OH does not emit within the spectral window selected). The 150°C TL emissions are correlated to the existence of germanium impurities. The high temperature emissions are not totally interpreted, nevertheless the luminescence community admits that the 325°C TL emission is produced by the thermal evaporation of a hole initially trapped onto an aluminium center (with an alcali ion in the vicinity). Concerning the TL emissions around 400°C and above, they could accompany the thermal release of charges from OHC and/or peroxy type centres. The release of the electron trapped in an oxygen vacancy ( $E'$  center) would occur at

very high temperature (more than 500°C). The potential TL due to that mechanism is not observable with our device.

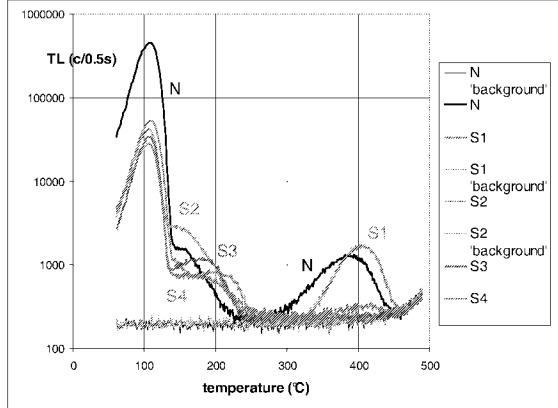


Figure 16. TL response of natural (N) and synthetic quartz (S1 to S4) irradiated by 10 Gy. Differences in shapes with TL of highly irradiated quartz result in dose effects,  $\beta$  and  $\gamma$  radiations leading to the same ionizing mechanisms.

#### IV. CONCLUSION

Some solutions have been used to reduce partly USO radiation sensitivity : shielding, specific quartz materials and quartz crystal pre-conditioning. Even if they can be efficient, each of them has a drawback. Shielding does not guarantee total radiation protection (high energy protons) and weight criterion must be taken into account. Scattering observed on specific quartz materials force on-board USO manufacturer to evaluate LDR radiation performances of each quartz crystal resonators of a production batch. Furthermore, this heavy operation does not guarantee the low LDR sensitivity. And, if the pre-conditioning operation allowed to improve this LDR sensitivity, this step of the USO development is so heavy.

Because of these drawbacks, CNES and French experts in radiation and in quartz material and oscillator have been gathered to determine and understand the mechanisms responsible of the radiation sensitivity of material and oscillator and to correlate them in order to reduce their susceptibility.

Various measurements have been done. All the experiments envisaged are not yet achieved (particularly with a very high dose of  $\gamma$ -rays), but we can now create a hierarchy between the 4 synthetic samples and clearly classify the S2 at the top of our classification and the natural one at the end: the last one contains the more mobile charge carriers. We confirm that, if the dislocations can help the mobility of charge carriers, they are not necessary (than in natural quartz) to promote this mobility. The charge carriers are displaced along the C-axis channels, like during sweeping.

Our last step will be to compare these results to the frequency shift of resonators built in the same materials than those studied under irradiation.

#### V. ACKNOWLEDGMENT

Authors thank JF-Dutrey from CNES and J-P. Roman from LCEP dept. and SHIVATECnologie for their technical supports, G. Villeneuve and R. Chapoulie for their contributions from CRP2A and M. Brunet initiator of this R&D.

#### REFERENCES

- [BAH99] Bahadur H. "Hydrogen and its radiation effects in quartz crystals," Proc. Of EFTF and IEE-IFCS, pp.777, 780, 1999.
- [BRU05] Brunet M., Cibiel G., Ecoffet R., Rolland G., Boy JJ., "Space radiation effects on ultra stable oscillators," EFTF 2005
- [CAN95] Candelier V., Lamboley J., Marotel G., Canzian P., Poulain P., "Recent progress in ultra stable oscillators for space on-board and ground applications," Proc. Of EFTF, pp. 325-331, 1995
- [DEV99] Devautour S., Henn F., Giuntini J.C., Zanchetta J.V. and Vanderschueren J., "TSDC relaxation map analysis in a Na-mordenite zeolite", Solid State Ionics, Vol 122, pp 105-111, 1999.
- [FOT73] Fotchenkov A.A., Kolodieva S.V., "Some features of the action of penetrating radiation on the electrical properties of a quartz crystal". Soviet-Physics-Crystallography, 366-9, 1973 .
- [HAS97] Hashimoto T., Katayama H., Sakaue H., Hase H., Arimura T., Ojima T., "Dependence of some radiation induced phenomena from natural quartz on hydroxyl-impurity contents," Radiation Measurements, 1997, 27, 243-250.
- [JEA92] Jeandel G., Warin A., Poignon C., Aubry JP, Morlot G.. "Mesure de courants thermoioniques dans le quartz", 6<sup>th</sup> European Frequency and Time Forum Noordwijk, 17-19 march 1992
- [MAR96] Martin JJ., "estimation of aluminium and growth-defects contentin cultured quartz by using infrared absorption", Proc. Of IEE IFCS, pp. 126-130, 1996.
- [MAR02] Martin J.R., Croxall D.F., McGovern M., Haston A.L., "The growth of high quality purity quartz in heavy water," Proc. Of IEEE IFCS, pp. 354 - 360, 2002
- [NOR84] Norton J.R., Cloeren J.M. and Suter J.J., "Results from gamma ray and proton beam radiation testing of quartz resonators," Proc. Of IEEE Annual FCS, pp. 63 - 72, 1984
- [SEM85] Semenov K.P., Fotchenkov A.A., Kapustina G.A. "Radiation-induced defect formation in quartz. II. Correlation dependences of optical, acoustical, and dielectric properties." Soviet-Physics-Crystallography, 335-42, 1985.
- [SUT88] Suter J.J. "Acoustic loss and frequency stability studies of gamma and proton irradiated alpha quartz crystal resonators," Ph.D dissertation, John Hopkins University, Baltimore, 1998
- [STA84] Stassinopoulos E.G. and Barth J.M., "Transport and shielding analysis of the non-equatorial terrestrial low altitude charged particle radiation environment," NASA Technical Report X-601-84-6, Volume I, 1984
- [VIG94] Vig J.R. and Walls F.L., "Fundamental limits on the frequency instabilities of quartz crystal oscillators," Proc. Of IEEE IFCS, pp. 506 - 523, 1994
- [WEA04] Weaver G.L., Reinhart M.J., Brian Sequeira H. and Stapor W., "Examination of detailed frequency behavior resonators under low dose exposures to proton radiation," Proc. Of IEEE IFCS, pp. 356-364, 2004